Vacuum Ultraviolet Application of Li2B4O7 Crystals: Generation of 100 fs Pulses Down to 170 nm

doi: 10.1063/1.368904

Vacuum ultraviolet application of $Li_2B_4O_7$ crystals: Generation of 100 fs pulses down to 170 nm

V. Petrov,[a] F. Rotermund, and F. Noack
Max-Born-Institute for Nonlinear Optics and Ultrafast Spectroscopy, 6 Rudower Chaussee, D-12489 Berlin, Germany

R. Komatsu, T. Sugawara, and S. Uda
Advanced Technology Research Laboratories, Central Research Institute, Mitsubishi Materials Corporation, 1-297 Kitabukuro-cho, Omiya, Saitama 330, Japan

(Received 20 July 1998; accepted for publication 1 September 1998)

We investigate and characterize the newly grown crystal $Li_2B_4O_7$ which is transparent down to 160 nm for nonlinear optical conversion into the vacuum ultraviolet using sum frequency mixing with femtosecond pulses. This material exhibits excellent properties below 180 nm and makes possible the generation of wavelengths down to 170 nm with an all solid state laser system. The most important advantage of $Li_2B_4O_7$ in this spectral range turns out to be the possibility of utilizing noncritical phase matching with maximized effective nonlinearity. We demonstrate generation of nearly transform limited 100 fs pulses between 170 and 185 nm with conversion efficiency of 4%. Their peak powers range from 200 kW at 170 nm to >2 MW at 185 nm. © *1998 American Institute of Physics.* [S0021-8979(98)07523-9]

I. INTRODUCTION

There is currently much interest in borate crystals for development of all solid state laser systems in the vacuum ultraviolet (VUV) based on phase-matched second order nonlinear conversion processes. The most promising such scheme for generation of tunable VUV laser radiation relies on Ti:sapphire laser technology. Although Ti:sapphire lasers are tunable near 800 nm and several cascaded processes are necessary to move to the 200-nm-spectral region, high powers in the VUV and high conversion efficiencies can be achieved using short pulse Ti:sapphire laser sources. Femtosecond pulses are particularly suited for this purpose since besides the higher peak powers, their interaction is limited to relatively short temporal walkoff lengths and consequently thin crystals with better transparency properties near the VUV cutoff edge can be used.

Fourth harmonic (FH) of Ti:sapphire femtosecond laser systems can be generated down to 189 nm, which is the cutoff edge of β-barium borate BaB_2O_4 (BBO), the crystal with the largest birefringence among all VUV-transparent nonlinear crystals. Efficient conversion to the FH has been previously demonstrated both with Ti:sapphire regenerative amplifiers[1] and Ti:sapphire mode-locked oscillators.[2] For achieving even shorter wavelengths one has to apply sum frequency generation (SFG) using the FH and near-infrared (NIR) radiation.[3] Although well known crystals like KH_2PO_4 (KDP) and $NH_4H_2PO_4$ (ADP) are transparent below 190 nm, SFG below 190 nm is impossible with them since their NIR transmission is limited to ≈ 1.55 μm. The recently developed borate crystals lithium triborate LiB_3O_5 (LBO), cesium triborate CsB_3O_5 (CBO), and cesium lithium borate $CsLiB_6O_{10}$ (CLBO) seem all to have attractive properties for VUV applications below 190 nm. CLBO is transparent, however, only down to 180 nm and LBO and CBO both have vanishing effective nonlinearity in the limit of 90° noncritical phase matching.

In this work we characterize a newly developed nonlinear crystal of the borate family, lithium tetraborate $Li_2B_4O_7$ (LB4) for VUV applications. Large samples of this crystal have been successfully grown most recently by the Czochralski method with good homogeneity of the refractive index and few dislocations.[4] LB4 is negative uniaxial and belongs to the 4 mm point group which means that its effective nonlinearity is maximized under the conditions of 90° phase matching. The clear transmittance spans from 170 to 3300 nm. We demonstrate SFG of tunable VUV femtosecond pulses with LB4 from 185 nm down to 170 nm (7.3 eV), the lower limit being set by the available FH tunability. To the best of our knowledge these are the shortest wavelengths achieved with phase-matched frequency conversion in nonlinear optical crystals. A comparison with a LBO reference sample reveals that LB4 has a superior performance in the VUV spectral region below 180 nm.

II. CRYSTAL PROPERTIES AND PHASE MATCHING

In Table I we have summarized the important properties of all known borate crystals that can be used below 190 nm. The recent reports on $Sr_2Be_2B_2O_7$ (SBBO) and $KBe_2BO_3F_2$ (KBBF) (Ref. 5) are not included, because the application of these materials below 190 nm seems at present impossible as a consequence of difficulties in the growing and cutting process. Instead of some average value for the birefringence we have included in Table I, the minimum achievable second harmonic (SH) and FH wavelengths which are good criteria to compare the phase-matching properties of the different crystals. The point of minimum SH (or FH) wavelength is

[a]Electronic mail: petrov@mbi-berlin.de

TABLE I. Nonlinear optical crystals applicable for SFG below 190 nm. θ and φ denote the polar and azimuthal angles, respectively. The minimum FH wavelength is estimated for SFG between the fundamental and the third harmonic. The transparency is given for the zero level transmission.

NLO crystal type point group, axes	Transparency (μm)	Effective nonlinearity best Sellmeier expansion (Ref.)	Nonlinear coefficient (pm/V)	Minimum SH and FH wavelengths, both achieved at
LBO (LiB_3O_5) negative-biaxial (mm2) $x,y,z:a,c,b$	0.155–3.2	$d_{ooe}=d_{32}\cos\varphi$ (Ref. 6)	$d_{32}=0.85$	277 nm 242.5 nm $\theta=90°,\ \varphi=90°$ $d_{\text{eff}}=0$
CBO (CsB_3O_5) positive-biaxial (222) $x,y,z:c,a,b$	0.167–3.0	$d_{eeo}=d_{14}\sin 2\theta$ (Ref. 7)	$d_{14}=1.08$	272.8 nm 236.3 nm $\theta=90°,\ \varphi=90°$ $d_{\text{eff}}=0$
CLBO ($CsLiB_6O_{10}$) negative-uniaxial (42m)	0.18–2.75	$d_{ooe}=d_{36}\sin\theta\sin 2\varphi$ (Ref. 8)	$d_{36}=0.86$	236 nm 209.5 nm $\theta=90°,\ \varphi=45°$ $d_{\text{eff}}=d_{\max}$
KB5 ($KB_5O_8.4H_2O$) positive-biaxial (mm2) $x,y,z:c,b,a$	0.162–1.5	$d_{ooe}=d_{31}\sin\varphi$ $d_{eeo}=d_{31}\sin^2\theta+d_{32}\cos^2\theta$ (Ref. 9)	$d_{31}=0.04$ $d_{32}=0.003$	217 nm 194.8 nm $\theta=90°,\ \varphi=90°$ $d_{\text{eff}}=d_{\max}$
LB4 ($Li_2B_4O_7$) negative-uniaxial (4mm)	0.16–3.6	$d_{ooe}=d_{31}\sin\theta$ (Ref. 10)	$d_{31}=0.12$	243.8 nm 218.3 nm $\theta=90°$ $d_{\text{eff}}=d_{\max}$

achieved at $\theta=90°$ for uniaxial crystals and along the y axis ($\theta=90°,\ \varphi=90°$) for the biaxial crystals. These orientations coincide of course with the propagation directions for minimum SFG wavelengths. The effective nonlinearity is given in Table I only for the best choice configuration, i.e., for the interaction scheme providing the shortest SH (or SFG) wavelength. Note that in the case of KB5 the SH minimum point can be reached with the same polarization configuration both in the $x-y$ and the $y-z$ planes, but for tunable operation, propagation in the $y-z$ plane ($ee\rightarrow o$) seems preferable since it requires smaller changes in the critical angle θ. The main problem with LBO and CBO as can be seen from Table I is the vanishing effective nonlinearity when propagating along the y axis. At longer VUV wavelengths (deviating from the 90° limit) CBO could provide higher efficiency than LBO but it is unclear if this material can have some advantages over LBO in the 90° limit. The birefringence of CBO is larger than that of LBO, but the predictions of the existing Sellmeier expansion (see Fig. 3 in Ref. 7) seem to deviate substantially from the experimental results in the 90° limit. It is obvious that CLBO has greater potential than LBO for effective frequency conversion below 190 nm but unfortunately its cutoff edge is at 180 nm. In this crystal, in contrast to all other borates included in Table I, the lower VUV limit when using the SFG scheme mentioned in Sec. I is set by the transparency cutoff edge and not by the birefringence (phase matching). That is why 90° phase matching is never reached with type-I interaction below 190 nm and it is possible in principle to use CLBO also with type-II ($eo\rightarrow e$) interaction in order to improve the conversion efficiency.

The new nonlinear material LB4 on the other hand has smaller nonlinear coefficient but its effective nonlinearity is maximum at $\theta=90°$. LB4 was originally proposed as a substrate for surface acoustic wave devices.[11] Its nonlinear optical coefficients were estimated in Ref. 12 (see Table I) and the SH generation of a Nd:YAG laser (1064 nm) was studied in more detail in Ref. 13. Most recently LB4 proved to be very promising for the generation of the fourth and fifth harmonics of Nd:YAG lasers.[4] As observed in Ref. 4 the hygroscopicity of LB4 is less than for the other borate crystals. From Fig. 1 it can be seen that the short wave cutoff for thin samples is below 160 nm. For the evaluation of the phase-matching properties of LB4 in the VUV we used the following Sellmeier expansion:[10]

$$n_0^2=2.564\,31+\frac{0.012\,337}{\lambda^2-0.013\,103}-0.019\,075\lambda^2,$$
$$n_e^2=2.386\,51+\frac{0.010\,664}{\lambda^2-0.012\,878}-0.012\,813\lambda^2, \tag{1}$$

where the wavelength λ is in μm. The birefringence of LB4 is higher than that of LBO but smaller than the birefringence of the well known material KB5. This can also be seen in Fig. 2 which shows that SFG in LB4 requires NIR wavelengths longer than in KB5 and shorter than in LBO in order to fulfill the phase-matching condition for a given VUV wavelength λ_3. KB5 is, however, a soft hygroscopic crystal

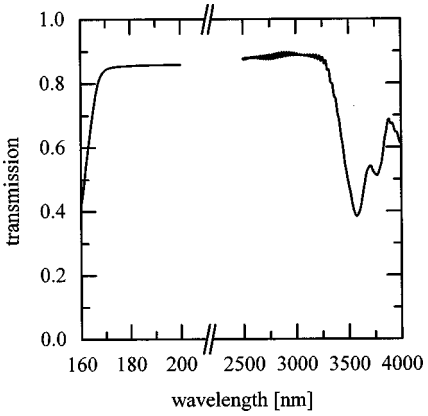

FIG. 1. VUV and midinfrared cutoff edges of a 107-μm-thick sample of LB4 ($\theta=80°$ cut) recorded with unpolarized light.

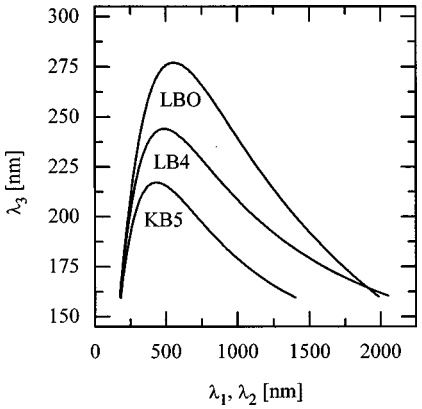

FIG. 2. Noncritical (90°) type-I phase matching for SFG in LBO, LB4, and KB5. We use the convention $\lambda_1 > \lambda_2 > \lambda_3$ and $1/\lambda_3 = 1/\lambda_1 + 1/\lambda_2$. The case $\lambda_1 = \lambda_2$ corresponds to SH generation and can be found in Table I. These curves are limited on both sides by the VUV cutoff edges.

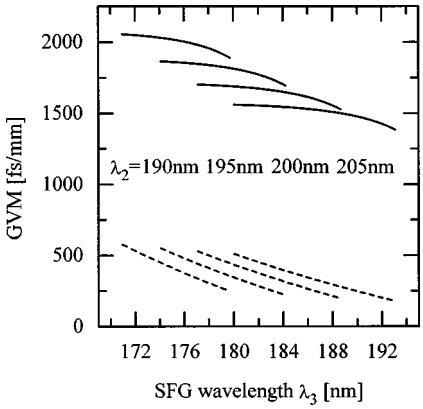

FIG. 4. Inverse group velocity mismatch (GVM) for VUV-SFG in LB4. $1/v_2 - 1/v_1$ (solid lines) and $1/v_3 - 1/v_2$ (dashed lines). The four FH wavelengths (λ_2) are indicated and correspond to the tuning ranges in Fig. 3.

with nonlinearity approximately three times lower than that of LB4 which makes it rather unsuitable for practical applications. We note only here that KB5 is the only crystal besides BBO that is partially phase matchable for FH generation of Ti:sapphire laser radiation (see Table I).

Synchronized femtosecond pulses at kilohertz repetition rates in the NIR for mixing with the FH can be generated by traveling-wave optical parametric generators pumped by the fundamental of Ti:sapphire regenerative amplifiers.[14] According to Fig. 2 the idler output can be used as λ_1 for SFG in LBO and LB4, and the signal output is suitable for SFG in KB5. Note that the use of optical parametric generators permits independent tunability of the FH (λ_2) and the signal or idler waves (λ_1) so that noncritical (90°) phase matching is always realizable. The critical (angle) tuning near 90° is shown for LBO and LB4 in Fig. 3. The chosen values for λ_2 correspond to typical FH wavelengths achievable with Ti:sapphire laser systems. It can be seen that the VUV limit in both crystals is determined not by VUV (or NIR) absorption but rather by the availability of the FH wavelengths. The latter in turn is not restricted by the tunability range of the Ti:sapphire laser systems, but by the absorption edge of BBO (at 189 nm) used to generate the FH.[1]

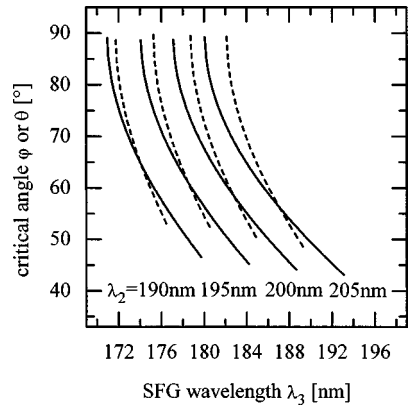

FIG. 3. Critical tuning for VUV-SFG in LBO (dashed lines) and LB4 (solid lines) for four values of the FH wavelength (λ_2) indicated. The tuning is achieved by the azimuthal angle φ in the x-y plane in LBO and by the polar angle θ in LB4. These curves are limited on the right-hand side by the NIR cutoff edges.

The calculated inverse group velocity mismatch in LB4 for the VUV spectral range is shown in Fig. 4. The large difference in the propagation velocities of the FH and NIR pulses poses an upper limit for the achievable VUV pulse duration (and also for the conversion efficiency) which depends on the specific values of the FH and NIR pulse durations. This parameter is used for estimation of the optimum crystal thickness L since the latter should not substantially exceed the interaction length between the FH and NIR pulses. Numerical simulations in the undepleted plane wave approximation assuming Gaussian-shaped FH and idler pulses of the same duration T reveal that the VUV pulse duration varies between 0.7 and 1.7 T when the crystal thickness changes from 0 to $2\,T/(1/v_2 - 1/v_1)$. At larger crystal lengths this dependence saturates. Thinner crystals have the additional advantage of providing enhanced transmission near the VUV cutoff edge. At a chosen or fixed crystal thickness L the actual pulse duration (not the upper limit) at the sum frequency is influenced also by the group delay of the emerging VUV wave relative to the FH and NIR pulses (Fig. 4).

III. EXPERIMENTAL SETUP

The experimental setup is shown in Fig. 5. It is similar to the one used previously by us,[3] the main difference consists in the NIR optical parametric generator which now possesses wavelength tunability that is much broader and independent of the pump wavelength. The commercial Ti:sapphire laser oscillator/regenerative amplifier (TRA-1000, CLARK) delivers 600 μJ, 100 fs pump pulses at 1 kHz repetition rate. It is equipped with a continuum seeded optical parametric generator (IR-OPA, CLARK). The latter is based on type-II interaction in BBO and consequently the generated idler wave can be easily separated by use of a polarizer (Fig. 5). Typical pulse durations at the idler wavelength measured by autocorrelation using SH generation are about 140 fs and the idler pulse energy amounts typically to 30 μJ. The idler tunability range (1.6–2.5 μm) depends only weakly on the pump wave-

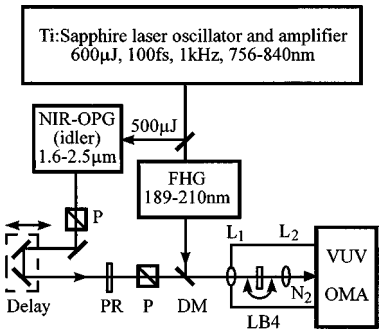

FIG. 5. Experimental setup. FHG: FH generation, NIR-OPG: NIR optical parametric generator, PR: waveplate, P: polarizers, DM: 193 nm, 45° excimer laser mirror, L1, L2: MgF_2 lenses of 10 cm focal length, VUV-OMA: VUV-optical multichannel analyzer.

length but is in any case sufficient for all interactions displayed in Fig. 3. The FH generation is based on a scheme described in detail in Ref. 1. It uses sequential frequency conversion in BBO crystals with group delay precompensations before the third and fourth harmonic stages. The FH pulse duration is of the same order as the idler pulse duration. After adjustment of parallel polarizations the FH and the idler waves are recombined by a dichroic mirror (DM, Fig. 5) for collinear SFG. The crystal used for VUV-SFG is mounted in an isolated chamber with nitrogen purging. The first focusing lens L_1 also serves as an entrance window and the second lens L_2 focuses the VUV beam onto the monochromator slit. The nonlinear crystal is positioned before the focal point of L_1 and both interacting beams have a Gaussian diameter of ≈ 170 μm in the position of the crystal. The 0.2-m-VUV monochromator (McPherson, Model 234/302) is equipped with a 1200 lines/mm grating. It is evacuated and with MgF_2 window in front of the entrance slit. The CCD VUV-optical multichannel analyzer (Spectroscopy Instruments, Model ST-130/TE-CCD-576) provides 0.06 nm/channel spectral resolution. The computer controlled delay line permits time delay adjustment and records of the cross correlation function between the FH and the idler waves.

The LB4 sample thickness (107 μm) chosen for the present experiment is comparable with the interaction length and accordingly no pulse broadening of the generated VUV pulses should be expected. At this crystal thickness clear transmission in the whole tunability range from Fig. 3 is available (see Fig. 1). The LB4 sample has a 10×10 mm clear aperture and is cut at $\theta = 80°$. A reference sample of LBO with 200 μm thickness is cut at $\theta = 90°$, $\varphi = 80°$ for propagation in the $x-y$ plane.

IV. RESULTS AND DISCUSSION

As can be seen from Table II we obtained rather good agreement between the calculated using (1) phase-matching angles for SFG in LB4 and the experimentally measured values. The discrepancies are larger only for $\theta > 80°$ where the accuracy of the experimental estimation when approaching the noncritical case and in particular when using broadband radiation (as is the case with femtosecond pulses) worsens. Thus we can conclude that the Sellmeier expansion (1) is applicable also in the VUV spectral range with sufficient precision. We compared the theoretical and experimental values for the angular acceptance at $\lambda_3 = 180$ nm. The experimentally measured full width at half maximum (FWHM) value (internal acceptance angle) of 2.7° is also in very good agreement with the calculated value of 2° again bearing in mind that we are dealing with relatively broad spectral widths.

TABLE II. Calculated (θ_{calc}) and observed (θ_{obs}) phase-matching angles with LB4 in the VUV.

λ_2 (nm)	λ_3 (nm)	θ_{calc} (deg)	θ_{obs} (deg)
205	183.8	65.6	66.1
200.5	180	69	69.5
198.3	177.5	74.3	75.8
195.7	175.26	78.3	80.4
192.9	173	83.5	89.8
190.4	171.5	82.4	≈90
189.5	171	82.5	≈90
189.14	170.75	81.7	≈90

Figure 6 shows the achieved tunability in the VUV when varying both the FH and idler wavelengths in the neighborhood of 90° phase matching. We note that the predictions of the Sellmeier expansion (1) for the shortest achievable VUV wavelength (about 170 nm) at the minimum FH wavelength of 189 nm are fulfilled by spectral components in Fig. 6. The spectral widths measured (FWHM) were of the order of 0.5 nm. Assuming a Fourier product of 0.5 (the same as the one measured for the FH pulses) we arrive at an estimation of about 100 fs for the duration (FWHM) of the VUV pulses. This figure is in good correspondence with simulations of the SFG process with 140 fs FWHM durations assumed at the FH and idler waves. As previously observed in other spectral regions we can also conclude in the VUV that choosing the crystal length comparable to the interaction length (see Fig. 4) results in pulse shortening and consequently lower efficiency than would be achievable with a longer crystal at the expense of reproducing the input pulse durations.

Another evidence for the pulse shortening taking place in the LB4 crystal is the recorded cross correlation functions in Fig. 7 where we have plotted the VUV pulse energy as a

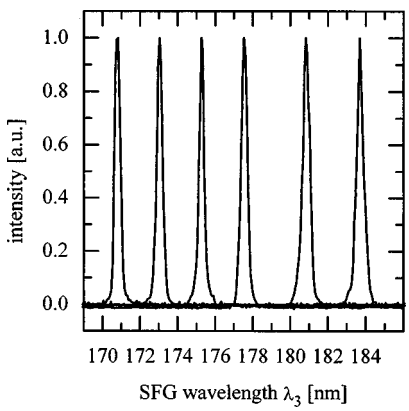

FIG. 6. VUV spectra obtained by SFG in LB4 demonstrating the achieved tunability.

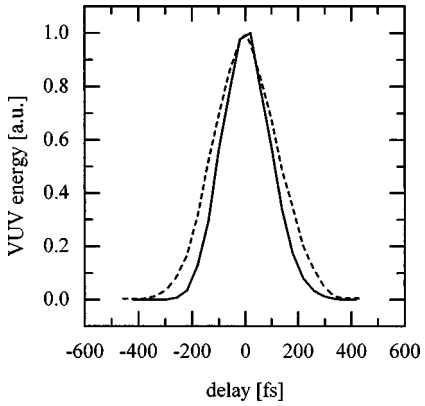

FIG. 7. Relative energy of the generated VUV pulse obtained with the LB4 crystal in dependence on the delay between the FH and idler pulses at $\lambda_3 = 180$ nm for $\lambda_2 = 201$ nm (solid line) and at $\lambda_3 = 170.75$ nm for $\lambda_2 = 189$ nm (dashed line).

function of the delay between the FH and idler pulses. The lack of any plateau in these curves indicates that the interaction length is not substantially shorter than the actual crystal length. Thus the measured curves can serve as reliable cross correlation measurements of the idler pulse duration knowing the FH pulse duration and vice versa. The measured FWHM of the solid curve in Fig. 7 amounts to 220 fs and is in very good agreement with what one would expect with the typical widths of 140 fs for the FH and idler pulses assuming Gaussian temporal shapes. This was confirmed by numerical simulations of the SFG taking into account the group delay in the LB4 crystal. The dashed curve in Fig. 7 was recorded at the lower limits for the FH and VUV wavelengths. Its FWHM of 280 fs is broader which is attributed in part to the increased GVM between the FH and NIR pulses in the LB4 crystal (see Fig. 4) and in part to lengthening of the FH pulse in the limit of the BBO transmission. Both effects are expected to have only weak (<20%) influence on the VUV pulse duration.

We compared the results obtained with the LB4 crystal with those obtained by substituting it by the LBO reference crystal. Correcting for the different crystal lengths we conclude that LBO provides higher efficiency only down to $\lambda_3 = 180$ nm. At shorter VUV wavelengths LB4 showed superior results. The predictions of Fig. 3 concerning the minimum VUV wavelengths achievable with LBO could not be confirmed. Although the calculated minimum VUV wavelength at $\lambda_2 = 189$ nm is $\lambda_3 = 171$ nm we could achieve VUV wavelengths only down to 172.7 nm reproducing our previous result.[3] This discrepancy is caused by several factors. First of all we found out that the Sellmeier expansion for LBO[6] predicts lower phase-matching angles φ that the measured ones. Thus, e.g., we measured 2.3° deviation at $\lambda_3 = 180$ nm and $\lambda_2 = 200.7$ nm and 5° deviation at $\lambda_3 = 176.4$ nm and $\lambda_2 = 195.3$ nm. These differences are obviously larger than those observed with LB4 in Table II. We note that 2°–6° larger experimental phase-matching angles were previously observed in the 195–188 nm spectral region with LBO in Ref. 15 and similar results were tabulated also in Ref. 16. This means that the best Sellmeier coefficients for LBO[6] could still be improved in the VUV. In addition we clearly observed spectral shifting with LBO towards longer wavelengths in the 90° limit (deviation of the measured VUV wavelength from the one calculated from the central FH and idler wavelengths). This effect is attributed to selective conversion of only parts of the idler and FH spectra. The latter is possible since both interacting fields are broadband. The reason for the spectral shifting is the vanishing effective nonlinearity of LBO in the 90° phase-matching limit. The maximized effective nonlinearity of LB4 in this limit and the larger birefringence of LB4 are the factors contributing to the superior performance of this new nonlinear material below 180 nm. Utilization of 90° phase matching on the other hand provides the characteristic advantages of noncritical interaction like large angular acceptance and the lack of spatial walkoff.

The absolute measurement of the VUV pulse energy and the estimation of the conversion efficiency is quite a difficult task in this wavelength range. To improve the reliability of such measurements we performed them at relatively long wavelengths and transformed the results to shorter VUV wavelengths since the geometry was held constant during this experiment. Direct mounting of an energy meter at the exit of the evacuated monochromator was not possible so we removed the nitrogen purged chamber and performed an absolute measurement of the VUV energy at $\lambda_3 = 184$ nm. At this VUV wavelength the beam could be easily separated from the FH by a suprasil prism and the influence of the air absorption could be estimated by variation of the separation to the detector. For the energy measurement we used a Si-:photodiode with removed window which was calibrated using the FH at 189 nm and a pyroelectric energy meter. Assuming equal response at 189 and 184 nm we measured first the efficiency with LBO since at 184 nm it worked better than LB4. The conversion efficiency with LB4 was estimated then by comparing the outputs with LBO and LB4 using again the purged chamber and the VUV-OMA and choosing a VUV wavelength (180 nm) were both crystals gave similar outputs. Finally the estimation was recalculated for the 90° case ($\lambda_3 \approx 171$ nm) in LB4 taking into account the angle change as in the previous step. The result for the efficiency $\eta = E_3/E_2$ where $E_{3,2}$ denotes the VUV and FH energies was 4% at an incident idler energy $E_1 = 20\ \mu$J. Taking into account the available FH pulse energies with this system[1] we estimate in such a way peak powers in the VUV as high as 1.6, 0.8, and 0.2 MW at 180, 175, and 171 nm, respectively.

The above result can be compared to theoretical estimations for the SFG efficiency in the undepleted plane wave approximation. In this case we have

$$\eta = \frac{E_3}{E_2} = \frac{8\pi^2 d_{\mathrm{eff}}^2 L^2}{\epsilon_0 c n_1 n_2 n_3 \lambda_3^2} I_1, \tag{2}$$

where I_1 represents an average intensity for the idler wave and $n_{1,2,3}$ denote the corresponding refractive indices. Focusing effects are neglected in Eq. (2) since the LB4 crystal is much thinner than the confocal parameters. Nevertheless, the Gaussian spatial and temporal distributions can be taken into account in Eq. (2) by defining

$$I_1 = \frac{E_1}{2T\pi w_0^2}, \tag{3}$$

where $2w_0$ is the Gaussian diameter of the idler beam and T is the idler pulse duration (FWHM intensity). Equation (3) contains, in fact, a reduction factor of 4 as compared to the peak on-axis intensity. For $d_{\mathrm{eff}}(\theta=90°)=d_{31}$ we corrected the value of 0.12 pm/V from Ref. 12 which was estimated for 1.064 μm SH generation to our case using the Miller's rule and obtained $d_{\mathrm{eff}}\approx 0.21$ pm/V. Using this value for the effective nonlinearity and taking into account the Fresnel losses we obtained a theoretical estimation for the conversion efficiency about five times higher than the experimental result. One possible reason for this discrepancy could be two-photon absorption in the LB4 crystal. However, the lack of asymmetry in our time delay measurements in Fig. 7 indicates that this possibility can be ruled out under our experimental conditions at least at the VUV wavelengths. Intensity dependent transmission at the FH wavelength which is much more intense could not be observed either. The measured angular acceptance in the vicinity of 90° phase matching is also much larger than the beam convergence onto the crystal and should not affect the conversion efficiency. Another possible reason remains the spectral acceptance. For our crystal thickness the spectral acceptance is sufficient if we deal with bandwidth limited pulses, but the idler pulses are in general 1.5–2 times Fourier limited. This cannot fully account for the above discrepancy. A further possibility especially when dealing with new materials is always related to the exact value of the nonlinear coefficient which has still to be reconfirmed.[10,12,13] Nevertheless, having in mind the precision of our measurement we find the agreement between theory and experiment concerning the efficiency still reasonable.

V. CONCLUSION

In conclusion we have demonstrated the unique potential of the new nonlinear material LB4 for VUV frequency conversion down to the 170–180 nm spectral region. It can serve as a basis for relatively simple all-solid state systems in this spectral range starting with femtosecond Ti:sapphire laser amplifiers. The conversion efficiency reported could be further increased by applying tighter focusing since LB4 has a higher damage threshold than LBO[4] or by increasing the crystal length at the expense of pulse broadening. Therefore, in general, higher conversion efficiencies than those obtainable with third-order nonlinear processes in gases (0.01%–1%) can be expected. An additional unique feature of the present method of SFG for VUV short pulse generation is that it can be extended to quasi-cw mode-locked Ti:sapphire laser oscillators operating at 100 MHz. In this case efficient FH generation has already been demonstrated[2] and the traveling wave optical parametric generator used in the present work can be substituted by synchronously pumped optical parametric oscillators which are also commercially available. Further ultrafast applications of LB4 include down conversion of VUV radiation with thin samples for simple cross-correlation measurements of femtosecond pulses in this spectral range.

The lower limit of 170 nm achieved in the present work is set on one hand by the birefringence of LB4 and on the other hand by the lower wavelength limit of the FH. We believe that even shorter wavelengths down to the cutoff edge at 160 nm could be produced if shorter wavelengths at the FH would be available. Finally we note that the present system is unique not only with respect to the tunability range, but it provides also $\approx$100 fs short pulses there with peak powers in excess of 100 kW. These pulses are synchronized to a number of other pulses at different wavelengths and can serve as a basis for time-resolved pump and probe experiments in the VUV with kHz repetition rate.

[1] J. Ringling, O. Kittelmann, F. Noack, G. Korn, and J. Squier, Opt. Lett. **18**, 2035 (1993).
[2] F. Rotermund and V. Petrov, Opt. Lett. **23**, 1040 (1998).
[3] F. Seifert, J. Ringling, F. Noack, V. Petrov, and O. Kittelmann, Opt. Lett. **19**, 1538 (1994).
[4] R. Komatsu, T. Sugawara, K. Sassa, N. Sarukura, Z. Liu, S. Izumida, Y. Segawa, S. Uda, T. Fukuda, and K. Yamanouchi, Appl. Phys. Lett. **70**, 3492 (1997).
[5] C. Chen, Y. Wang, Y. Xia, B. Wu, D. Tang, K. Wu, Z. Wenrong, L. Yu, and L. Mei, J. Appl. Phys. **77**, 2268 (1995).
[6] K. Kato, IEEE J. Quantum Electron. **30**, 2950 (1994).
[7] K. Kato, IEEE J. Quantum Electron. **31**, 169 (1995).
[8] N. Umemura and K. Kato, Appl. Opt. **36**, 6794 (1997).
[9] N. Umemura and K. Kato, Appl. Opt. **35**, 5332 (1996).
[10] T. Sugawara, R. Komatsu, and S. Uda, Solid State Commun. **107**, 233 (1998).
[11] R. W. Whatmore, N. M. Shorrocks, C. O'Hara, F. W. Ainger, and I. W. Young, Electron. Lett. **17**, 11 (1981).
[12] S. Furusawa, O. Chikagawa, S. Tange, T. Ishidate, H. Orihara, Y. Ishibashi, and K. Miwa, J. Phys. Soc. Jpn. **60**, 2691 (1991).
[13] T. Y. Kwon, J. J. Ju, J. W. Cha, J. N. Kim, and S. I. Yun, Mater. Lett. **20**, 211 (1994).
[14] V. Petrov, F. Seifert, O. Kittelmann, J. Ringling, and F. Noack, J. Appl. Phys. **76**, 7704 (1994).
[15] A. Borsutzky, R. Brünger, and R. Wallenstein, Appl. Phys. B: Photophys. Laser Chem. **52**, 380 (1991).
[16] B. Wu, F. Xie, C. Chen, D. Deng, and Z. Xu, Opt. Commun. **88**, 451 (1992).